Computers & Fluids 65 (2012) 2–7

Contents lists available at SciVerse ScienceDirect

Computers & Fluids

journal homepage: www.elsevier.com/locate/compfluid

Runge–Kutta discontinuous Galerkin method for interface flows with a maximum preserving limiter

Erwin Franquet [a,b], Vincent Perrier [b,c,*]

[a] LaTEP-ENSGTI, Université de Pau et des Pays de l'Adour, Bâtiment d'Alembert, Rue Jules Ferry, 64 075 Pau Cedex, France
[b] INRIA Bordeaux Sud Ouest, CAGIRE Team, 351 Cours de la Libération, 33 405 Talence Cedex, France
[c] LMA-IPRA, UMR CNRS 5142, Université de Pau et des Pays de l'Adour, Avenue de l'Université, 64 013 Pau Cedex, France

ARTICLE INFO

Article history:
Received 9 January 2012
Accepted 23 February 2012
Available online 10 March 2012

Keywords:
Multiphase flows
Diffuse interface method
Discontinuous Galerkin method
Maximum preserving limiter
Rayleigh–Taylor instability

ABSTRACT

We propose a high order diffuse interface method for dealing with compressible multiphase flows with interfaces. This scheme is based on the discontinuous Galerkin formulation of Franquet and Perrier [1]. As it is linear, this scheme is oscillating, so that the volume fraction can become negative or greater than 1. For stabilizing it, the maximum preserving limiter introduced in Zhang et al. (2012) [2] is used. The scheme is applied to the computation of a Rayleigh–Taylor instability.

1. Introduction

This article is concerned with the approximation of multiphase compressible flows with a high order method. We will only deal with interface problems, in which all the interfaces are solved, which means that all the cells of the mesh are sufficiently small for capturing interfaces. For approximating such flows, many methods are possible, each one having their advantages and drawbacks. They can be divided into two families: sharp interface methods and diffuse interface methods. In sharp interface methods, the interfaces are represented as discontinuities, e.g. as the zero of a Level Set function in Level Set methods, where the Level Set function is an additional unknown of the system [3], or as a reconstructed discontinuity in the case of Volume Of Fluid methods [4], which is moved for example by a Lagrange and projection method. The main drawback of the sharp interface method is the possible difficulty in its implementation (e.g. VOF method in three dimensions on unstructured meshes), or their nonconservative formulation (Level-Set functions), which can be a major drawback when dealing with hyperbolic systems [5]. In diffuse interface methods, the pure phases are determined by a color function which is equal to 1 or 0, depending in which phase we are. This color function is moved by an *ad hoc* method, and is allowed to diffuse, so that the color function takes all the values between 0 and 1. The major drawback in diffuse interface methods is the numerical diffusion which can lead to a very bad representation of the interfaces, especially when long time computations are needed.

A way to circumvent the numerical diffusion is to use a higher order method, and in this article, we are interested in discontinuous Galerkin methods. These methods have already been derived for Level Set methods in [6], in which both the Hamilton–Jacobi equation for the Level Set function and the Euler system for the conservative variables are discretized by a discontinuous Galerkin method. Our approach is different, because here, both the interface and the conservative variables are described by a single hyperbolic model. This model, which is similar to the Baer and Nunziato one will be described in Section 2. The major difficulty for this type of model is its nonconservativity, therefore raising a problem in the definition of discontinuities. In [7], a general framework for discretizing nonconservative hyperbolic systems was found. This was applied in [8] for multiphase flows when the jump relations of the system are supposed to be known. In this article, we propose to test the method developed in [1], in which we developed a discontinuous Galerkin formulation of Abgrall and Saurel [9]. This scheme is described in Section 3. The main challenge for interface flow with an oscillating high order method is to ensure that the color function is always between 0 and 1. This is achieved by using the maximum preserving limiter introduced by Zhang et al. [2]. The numerical results are presented in Section 4.

2. Model

Two phase flows can be described by the Baer and Nunziato system [10].

* Corresponding author at: INRIA Bordeaux Sud Ouest, CAGIRE Team, 351 Cours de la Libération, 33 405 Talence Cedex, France.
E-mail address: vincent.perrier@inria.fr (V. Perrier).

0045-7930/$ - see front matter © 2012 Elsevier Ltd. All rights reserved.
http://dx.doi.org/10.1016/j.compfluid.2012.02.021

$$\begin{aligned}
&\frac{\partial \alpha_k}{\partial t} + \mathbf{u}_i \cdot \nabla \alpha_k = \mu(P_k - P_{\bar{k}}) \\
&\frac{\partial (\alpha_k \rho_k)}{\partial t} + \operatorname{div}(\alpha_k \rho_k \mathbf{u}_k) = 0 \\
&\frac{\partial (\alpha_k \rho_k \mathbf{u}_k)}{\partial t} + \operatorname{div}(\alpha_k \rho_k \mathbf{u}_k \otimes \mathbf{u}_k) + \nabla(\alpha_k P_k) = P_I \nabla \alpha_k + \lambda(\mathbf{u}_{\bar{k}} - \mathbf{u}_k) \\
&\frac{\partial (\alpha_k \rho_k E_k)}{\partial t} + \operatorname{div}(\alpha_k (\rho_k E_k + P_k)\mathbf{u}_k) = P_I \mathbf{u}_I \cdot \nabla \alpha_k - \mu P_I (P_k - P_{\bar{k}}) + \lambda \mathbf{u}_I (\mathbf{u}_{\bar{k}} - \mathbf{u}_k)
\end{aligned} \tag{1}$$

where the subscript k refers to the phase, which is equal to 1 or 2. α_k is the volume fraction of the phase k, ρ_k is the density of the fluid k, P_k its pressure, and $\mathbf{u}_k$ its velocity. The total energy E_k is defined by $E_k = \varepsilon_k + \frac{1}{2}|\mathbf{u}_k|^2$, where ε_k is the specific internal energy, linked with the other thermodynamic parameters of the fluid by an equation of state, $\varepsilon_k = \varepsilon_k(P_k, \rho_k)$. P_I and $\mathbf{u}_I$ are the pressure and velocity at the interface. For closing the system, these variables must be defined. Many choices are possible, for example if the first phase is light and very compressible, and the second phase is heavy and slightly compressible, $\mathbf{u}_I = \mathbf{u}_2$ and $P_I = P_1$ can be chosen [10]. Last, λ and μ are relaxation parameters, which will be supposed to be equal to 0.

3. Numerical method

The system (1) is hyperbolic, but cannot be put in a conservative form. As a consequence, jump relations across shocks cannot be defined directly with the system. One way to circumvent this problem is to impose an algebraic relation defining the shocks [11]. Solutions of the Riemann problem for (1) have been proposed for example in [12]. A general formulation of discontinuous Galerkin method for nonconservative problems has been derived in [7]. By combining it with explicit solution of the Riemann problem [8] applied this method to multiphase flows. Note that these references deal only with the Baer and Nunziato closure $\mathbf{u}_I = \mathbf{u}_2$ and $P_I = P_1$.

In this article, a different approach will be followed: the system (1) is the result of the averaging of the Euler system, see [13]. Following [9], we will restart from the Euler system, discretize it, and then average it.

3.1. Formulation of the scheme

Following [9,13], χ_k denotes the characteristic function of the phase k: $\chi_k(\mathbf{x}) = 1$ if the fluid k is on $\mathbf{x}$, $\chi_k = 0$ otherwise. Then the following set of equations holds

$$\chi_k(\partial_t \mathbf{U}_k + \operatorname{div}\mathbf{F}_k(\mathbf{U}_k)) = 0 \quad \partial_t \chi_k + \mathbf{u}_i \cdot \nabla \chi_k = 0$$

where $\mathbf{U}_k$ and $\mathbf{F}_k$ respectively denote the conservative variables and the conservative flux of the Euler equations. The first equation means that if the fluid k is present, it follows the Euler equations. The second one is an advection equation for χ_k, with velocity $\mathbf{u}_i$, which can be defined by the interfacial velocity of the solution of the Riemann problem between the fluid $\bar{k}$ and the fluid k in the direction of $\nabla \chi_k$. Combining these two equations leads to

$$\frac{\partial \chi_k \mathbf{U}_k}{\partial t} + \operatorname{div}(\chi_k \mathbf{F}_k(\mathbf{U}_k)) - (\mathbf{F}_k(\mathbf{U}_k) - \mathbf{u}_i \mathbf{U}_k)\nabla \chi_k = 0 \tag{2}$$

As explained in [13], averaging of (2) may lead to the system (1).

Let us consider now an open set Ω meshed by a conforming mesh $\mathcal{T}_h$. We define one unitary normal $\mathbf{n}$ on each side $S \in S_t$ of $\mathcal{T}_h$, where the set of sides $S_t = S_i \cup S_b$ involves interior sides S_i and boundary sides S_b. Applying the framework of Rhebergen et al. [7], we find in [1] the following DG formulation (*without* numerical fluxes), which has been averaged among the different flow topologies:

$$\begin{aligned}
&\frac{\partial \mathbb{E}\{\chi_k \mathbf{U}_k\}}{\partial t} + \sum_{K \in \mathcal{T}_h} \int_K -\mathbb{E}\{\chi_k \mathbf{F}(\mathbf{U})\}\nabla\varphi + \varphi(\mathbb{E}\{(\mathbf{F} - \mathbf{u}_i \mathbf{U})\nabla \chi_k\}) && (3) \\
&\quad - \sum_{S \in S_i} \int_S [\![\varphi]\!]\{\!\{\mathbb{E}\{\chi_k \mathbf{F}_k(\mathbf{U}_k)\}\!\}\} \cdot \mathbf{n}^S && (4) \\
&\quad + \sum_{S \in S_i} \int_S \{\{\varphi\}\} \int_0^1 \frac{\partial \Phi}{\partial s}(s, u^L, u^R)\mathbb{E}\{(\mathbf{F}_k(\mathbf{U}_k) - \mathbf{u}_i \mathbf{U}_k)\nabla \chi_k\} \cdot \mathbf{n}^S && (5) \\
&\quad + \sum_{S \in S_b} \int_S \varphi \mathbb{E}\{\chi_k \mathbf{F}(\mathbf{U})\} \cdot \mathbf{n}^{\text{out}} = 0 && (6)
\end{aligned}$$

where Φ is a path connecting the left state L and the right state R (see [11] for its definition), with $[\![\varphi]\!] = \varphi^R - \varphi^L$ and $\{\!\{\varphi\}\!\} = \frac{\varphi^R + \varphi^L}{2}$, and where $\mathbb{E}$ is a mathematical expectancy. This is an average of all the possible topologies of flows χ_k whose expectancy is equal to the volume fraction $\alpha_k(\mathbf{x})$. As in [1], we suppose that

$$\chi_1 = \frac{1 + \operatorname{sgn}(g_{\mathbf{x}})}{2} \tag{7}$$

where $g_{\mathbf{x}}$ is a stochastic Gaussian process, with mean $m(\mathbf{x})$, variance 1, and autocorrelation function R, with $R'(0) = R''(0) = 0$. $m(\mathbf{x})$ is calibrated for having $\mathbb{E}\{\chi_1(\mathbf{x})\} = \alpha_1(\mathbf{x})$ on all continuity point of α_1.

3.1.1. Boundary integrals

In this paragraph, we apply [9] for the boundary fluxes because it avoids to explicitly derive the jump relations for the nonconservative products. We found in [1] for the terms (4) and (5):

$$\int_S [\![\varphi]\!]\{\!\{\mathbb{E}\{\chi_k \mathbf{F}_k(\mathbf{U}_k)\}\!\}\} \cdot \mathbf{n}^S \approx \int_S [\![\varphi]\!] \mathcal{F}^{k,\text{eul},+} \tag{8}$$

$$\begin{aligned}
&\int_S \{\{\varphi\}\} \int_0^1 \frac{\partial \Phi}{\partial s}(s, u^L, u^R)\mathbb{E}\{(\mathbf{F}_k(\mathbf{U}_k) - \mathbf{u}_i \mathbf{U}_k)\nabla \chi_k\} \cdot \mathbf{n}^S \\
&\quad \approx \int_S \varphi^L \mathcal{F}^{k,\text{lag},-} + \int_S \varphi^R \mathcal{F}^{k,\text{lag},+}
\end{aligned} \tag{9}$$

where $\mathcal{F}^{k,\text{eul},+}$ and $\mathcal{F}^{k,\text{lag},\pm}$ are average of Eulerian and Lagrangian fluxes that we detail now. The discretization of Abgrall and Saurel [9] is based on averaging the fluxes integrated from Riemann problems between pure fluids on a side. As depicted in Fig. 1, the first step to define the flux on a side is to solve the three possible Riemann problems. Then, these Riemann problems are integrated considering the various interfaces. For example in Fig. 1, the integration of the homogeneous Riemann problems lead to classical Eulerian fluxes whereas the integration of the heterogeneous Riemann problem strongly depends on the interfacial velocity: it leads to an Eulerian flux on the fluid that lies on the side and to a Lagrangian flux on both phases which is added on the cell in which the interface is. Last, all these fluxes are averaged by the occurrence's probability of each Riemann problem. In [1], we proved that modelling the multiphase flow by (7) gives the same weights as in [9, p. 373–376].

3.1.2. Cell integrals

Now, we are interested in the expression of the term (3). Usually, a continuous formulation of the system is known. Therefore, this step is straightforward. Here, on the contrary, we first defined the boundary integrals. Consequently, we have to find a continuous formulation of the problem which is consistent with our definition of the boundary integrals. Based on (7), we found in [1]:

$$\mathbb{E}\{(\mathbf{F}(\mathbf{U}) - \sigma \mathbf{U}) \cdot \nabla \chi_1\} = \begin{pmatrix} 0 \\ -P^\star(\nabla\alpha_1)\mathbf{n}(\nabla\alpha_1)\|\nabla\alpha_1\| \\ -u^\star(\nabla\alpha_1)P^\star(\nabla\alpha_1)\|\nabla\alpha_1\| \end{pmatrix} \tag{10}$$

where $\mathbf{n}(\nabla\alpha_1)$ is the unitary vector that has the same sense and direction as $\nabla\alpha_1$, $P^\star$ and $u^\star$ are the pressure and velocity at the interface of the Riemann problem with direction $\mathbf{n}$ (left state corresponding to fluid 2 and right state to fluid 1).

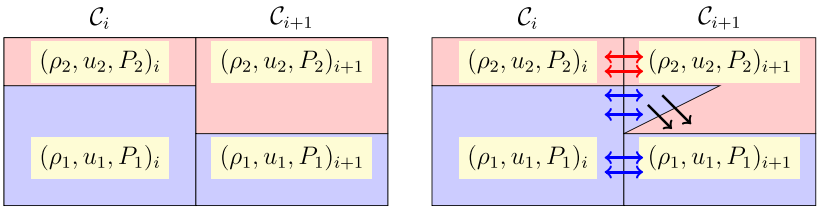

(a) Initial configuration. (b) Configuration after time evolution.

Fig. 1. Configuration of the Riemann problem on a side between two adjacent cells. Each cell is filled, area corresponding to the volume fraction, by fluid 1 (blue) or 2 (red). Given the initial configuration (a) three Riemann problems shall be considered: 1–1, 1–2 and 2–2. The Riemann problem 2–1 was not represented because its weight is zero. On (b) after solving the different Riemann problems, only the contact discontinuity between different materials is represented. Integration of homogeneous Riemann problems leads to classical Eulerian fluxes (blue and red arrows). In our case, concerning the heterogeneous Riemann problem, the blue fluid is entering the right cell. Thus its integration leads to an Eulerian flux on the side for the blue fluid and to a Lagrangian flux (black arrows) on both the blue and red fluids in the right cell (expressing the fact that the blue fluid is pushing the red fluid in the right cell).

3.2. Limitation

Discontinuous Galerkin methods are linear schemes, and are therefore oscillatory for nonlinear problems if their order is greater than 2. In our case, even when dealing with flows without shocks, this raises a problem, because interfaces are described by a volume fraction that must remain between 0 and 1.

An usual way to stabilize the scheme consists in combining explicit Runge–Kutta strong stability preserving schemes with a suitable slope limitation, see [14] and references therein. Nevertheless, most of the slope limiting are admittedly able to avoid oscillations around shocks, but are not able to preserve the maxima. Up to our knowledge, only the limitation introduced in [15], and then applied on triangular meshes in [2] is able to ensure that the variables remain bounded between two given values. We will first summarize this limiter, and then apply it to our system.

3.2.1. Maximum preserving limiter of Zhang et al. [2]

This limiter is based on two tricks.

1. Check that the maximum preservation is ensured for average of the variable on each cell.
2. Use a limiter local to the cell for limiting the moments of the variables, by a linear scaling around the cell average.

Actually, the maximum preservation is ensured only on the points that are used in the numerical method, namely the quadrature points of the boundaries of the cells for integrals (4) and (5), and quadrature points inside the cells (3). The proof of the step 1 was proved in [2] under a suitable CFL condition, provided a special quadrature formula is used for the cells: this quadrature formula is obtained by taking the Dubiner transformation of a tensor of a Gauss and Gauss–Lobatto quadrature formula, which is then symmetrized (see [2] for details). In Table 1, orders obtained for the cell integrals with such a quadrature formula are summarized. Following [14], the quadrature formula used for an approximation of degree k must be of degree $2k+1$ for the boundary integrals, and of degree $2k$ for the cell integrals. Therefore, the formula used comes from the product Gauss (1) × GaussLobatto (2) for degree 1, Gauss (3) × GaussLobatto (4) for degree 2, and Gauss (4) × GaussLobatto (5) for degree 3.

Table 1
Orders of the quadrature formula on a triangle, obtained by taking Dubiner's transformation of a tensor product of a Gauss and Gauss–Lobatto quadrature formula, and by symmetrizing it.

Gauss–Lobatto	Gauss					
	1	2	3	4	5	6
2	2	1	1	1	1	1
3	1	2	3	3	3	3
4	1	2	4	5	5	5
5	1	2	4	6	7	7
6	1	2	4	6	8	9

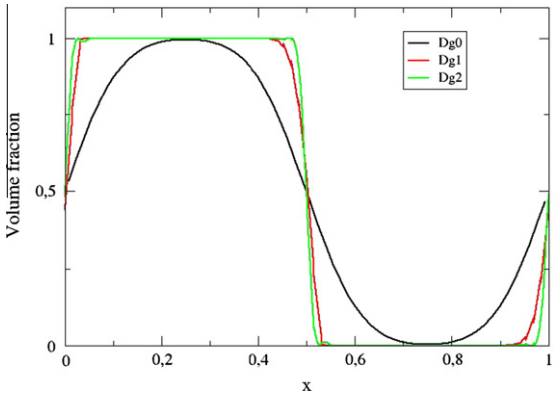

Fig. 2. Solution obtained for the advection of a one dimensional discontinuity on a mesh of 64 cells with approximation degree of 0, 1 and 2.

Once the maximum preservation is ensured on the average of the variables, and still following [2], the moments are limited by the linear scaling of Liu and Osher [16]: for a given polynomial $p_K(\mathbf{x})$ on the cell K, $\bar{p}$ denotes its cell average, and the moments are limited as follows

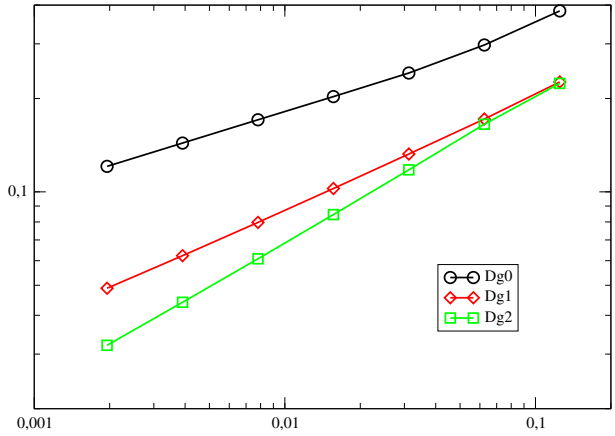

Fig. 3. Convergence error for the advection of a one dimensional discontinuity, represented on a log–log scale. We observe that the limiter used does not destroy the convergence order.

$$\tilde{p} = \theta(p - \bar{p}) + \bar{p} \quad \text{with} \quad \theta = \min\left\{\left|\frac{M-\bar{p}}{M_K-\bar{p}}\right|, \left|\frac{m-\bar{p}}{m_K-\bar{p}}\right|, 1\right\}$$

with $m_K = \min_{\mathbf{x}_i \in \mathcal{Q}_K} p_K(\mathbf{x}_i)$ and $M_K = \max_{\mathbf{x}_i \in \mathcal{Q}_K} p_K(\mathbf{x}_i)$, where $\mathcal{Q}_K$ denotes the set of the points of the quadrature formula on the cell K.

3.2.2. Application to the multiphase system

Following [1], the variables are limited as follows: if on the cell K and for one $i = 0$ or 1, $\alpha_K^{(i)}(\mathbf{x}) = 1$ for all $\mathbf{x}$ in K, then the cell is a pure fluid cell of fluid i. Its variables are limited by using a classical minmod limiter. Otherwise, if the cell is composed of two fluids, then there is an interface inside the cell. In this case, the volume fractions $\alpha_K^{(i)}$ are limited by using the maximum preserving limiter previously described above. The pure fluid variables (density, momentum, and total energy) are limited to their average, and the conservative variables of (1) are then reconstructed as follows: for example, the partial density $\alpha^{(i)}\rho^{(i)}$ is defined after limitation as

$$(\alpha^{(i)}\rho^{(i)})_K(\mathbf{x}) = \frac{\overline{\alpha\rho}_K^{(i)}}{\overline{\alpha}_K^{(i)}} \alpha_K^{(i)}(\mathbf{x})$$

3.3. How to take into account gravity

In our last numerical test, a Rayleigh–Taylor instability will be performed. In this case, a source term is added to the Euler equations, equal to $\rho\mathbf{g}$ for the momentum equation, where $\mathbf{g}$ (0, −9.81), and equal to $\rho\mathbf{g}\cdot\mathbf{u}$ for the total energy equation. If nothing is done, spurious oscillations can appear, because the stationary solutions are not conserved [17]: the scheme is not naturally well-balanced. A solution for well balancing discontinuous Galerkin methods was exposed in [18], nevertheless it is well suited with linearized Riemann solver, but not easy to adapt to exact Godunov' solver which we use. Here, the stationary solutions of the system with source term are simple: they are given by a vertical hydrostatic equilibrium where the velocity is equal to 0, the density is uniform, and the pressure is linked to the density, the gravity, and the ordinate y as $\Delta P = -\rho g \Delta y$. For ensuring the well balancing in the case of finite volume scheme, a local hydrostatic reconstruction can be made inside each cell: for a given cell with pressure P_0 and density ρ_0, the pressure on a point (x, y) of a cell with center (x_0, y_0) is defined as $P = P_0 - \rho g(y - y_0)$. With this definition it is straightforward to check that the scheme is well balanced. In the case of a higher order approximation, the scheme is naturally well balanced, because the source term is linear with respect to the conservative variables, and because the stationary solution is also linear with respect to y.

To summarize, the well balancing is achieved as follows.

- If the conservative variables of the pure fluid are constant inside a cell, which may happen when the global approximation is of degree 0, or when the slope limiting described previously is acting inside a cell with an interface, then an hydrostatic reconstruction is performed on the pure fluid variables.
- If the approximation degree is greater than 1, and if the cell is filled by a pure fluid, then the scheme is naturally well balanced.

4. Numerical results

In this section, we begin by performing numerical tests with two simple advection equations $\partial_t\alpha_k + \beta\cdot\nabla\alpha_k = 0$ with a given β. The aim is to see the benefit of high order, and the effect of the maximum preserving limiter on simple configurations. As far as the implementation is concerned, the system of Euler is replaced by an empty system, and the $u^\star$ used for advecting the volume fraction is replaced by the coefficient β of the equation we are dealing with. The second part of the numerical tests is dedicated to the simulation of a Rayleigh–Taylor instability.

4.1. Advection of a one dimensional discontinuity

This first test is made in one dimension. The computational domain is [0; 1] with periodic boundary conditions. For $x < 0.5$, α_1 is set to 1, whereas for $x > 0.5$, α_1 is set to 0. A uniform velocity of 1 is imposed. The computation is led until time 1. The solution obtained for a mesh of 64 cells is depicted in Fig. 2. The convergence order is shown in Fig. 3. It was proved in [2] that the maximum preserving limiter does not destroy the accuracy of the scheme for regular solutions. Of course, we do not find an order accuracy of 2 and 3 for the degrees 1 and 2 approximation, because the solution is not regular. Nevertheless, we can observe that the convergence order is not destroyed by the slope limiter.

4.2. Zalesak test

This test is taken from Ref. [19], and is very wide spread for testing numerical methods with interfaces, for example Level Set and Volume Of Fluid methods. The initial condition is a disk with a rectangular hole. The equation solved is an advection equation in which the velocity is a constant orthoradial velocity with respect to the center of the computational domain. Periodic boundary

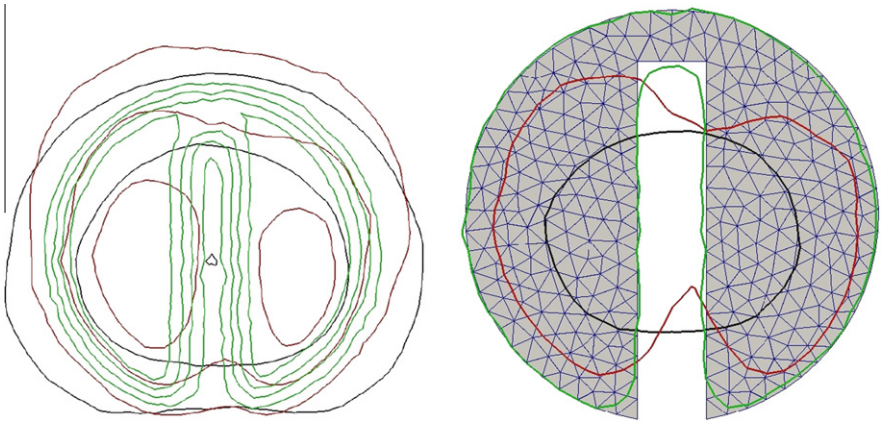

Fig. 4. Results for Zalesak test. On the left figure, we represented the isovalues 0.2, 0.4, 0.6 and 0.8 for the Dg0 (black), Dg1 (red) and Dg2 (green) computations. Note that some of these isovalues are not in the figure because they are too far from the initial shape. On the right side, we draw the isovalue 0.5 of α_1, and we compare it with the initial shape. These two figures prove the much stronger accuracy of the Dg2 computations, which is the only one able to conserve the initial shape.

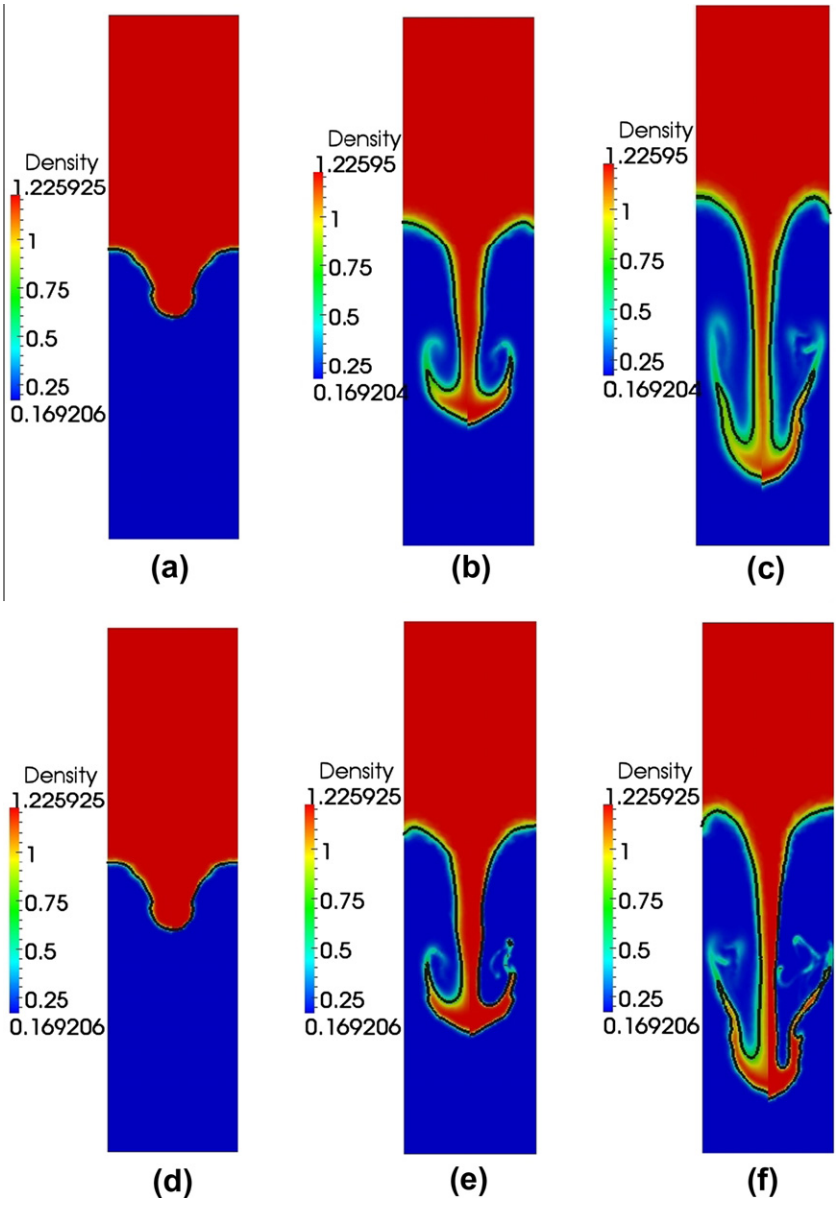

Fig. 5. Rayleigh–Taylor instability. Pictures (a)–(c) are a comparison of the $Dg0$ (left) and $Dg1$ (right) approximations, taken at time $t = 0.2$, $t = 0.6$, $t = 0.8$. Pictures (d)–(f) are comparisons between $Dg1$ (left) and $Dg2$ (right) at the same times.

conditions are imposed. The results obtained for this test are shown in Fig. 4.

4.3. Rayleigh–Taylor instability

The Rayleigh–Taylor instability consists in a superposition of a heavy fluid on the top of a lighter fluid, in presence of gravity. The computational domain is $[0;\ 0.5] \times [0;\ 4]$. The heavy fluid has a density of $\rho_h = 1.225$, and the light one a density equal to $\rho_l = 0.1694$. The interface between the fluids is located at $y_{\text{int}} = 2$. Both of the fluids are perfect gases, with the same γ parameter equal to 3. The pressure at the bottom is equal to $P_0 = 100$. The pressure is such that a hydrostatic equilibrium holds:

$$\begin{cases} P = P_0 - g\rho_l y & \text{if} \quad y \leqslant y_{\text{int}} \\ P = P_0 - g\rho_l y_{\text{int}} - g\rho_h (y - y_{\text{int}}) & \text{if} \quad y \geqslant y_{\text{int}} \end{cases}$$

The interface is perturbed by a cosine: $\tilde{y}_{\text{int}}(x, y) = y_{\text{int}} + 0.05\cos(2\pi x)$. The computation is led until time $t = 1$, with a mesh of 4932 triangles. Results are shown in Fig. 5. In the $Dg0$ and $Dg1$ computations, the appearance of the green[1] color emphasizes the diffusion of the density. The mushroom structure appears on the $Dg0$ computation, but no clear other structure appears there. A secondary structure appears in Fig. 5c. The $Dg2$ computation makes appear the detachment of a bubble of heavy fluid in Fig. 5e, but what is impressive is that the density is very low diffused for the $Dg2$ computation in Fig. 5f.

5. Conclusion

We presented a discontinuous Galerkin method for computing interfaces. This method combines the ideas of Abgrall and Saurel [9] and Rhebergen et al. [7], and result in a fully conservative scheme, which is high order accurate. The stabilization has been made with the slope limiter proposed by Zhang et al. [2], which allows to preserve the maximum on the volume fraction, but also to

[1] For interpretation of color in Figs. 1–5, the reader is referred to the web version of this article.

preserve the high order accuracy, as was proved in the numerical tests. Very good results were obtained with simple advection tests, but also on a Rayleigh–Taylor instability. The tests prove that the interface can be sharply resolved even with a diffuse interface method provided a high order scheme is used.

References

[1] Franquet E, Perrier V. Runge–Kutta discontinuous Galerkin method for the approximation of Baer and Nunziato type multiphase model. J Comput Phys. doi: 10.1016/j.jcp.2012.02.002. <http://dx.doi.org/10.1016/j.jcp.2012.02.002>.

[2] Zhang X, Xia Y, Shu C-W. Maximum-principle-satisfying and positivity-preserving high order discontinuous Galerkin schemes for conservation laws on triangular meshes. J Sci Comput 2012;50(1):29–62. http://dx.doi.org/10.1007/s10915-011-9472-8.

[3] Fedkiw RP, Aslam T, Merriman B, Osher S. A non-oscillatory Eulerian approach to interfaces in multimaterial flows (the ghost fluid method). J Comput Phys 1999;152(2):457–92. http://dx.doi.org/10.1006/jcph.1999.6236. <http://dx.doi.org/10.1006/jcph.1999.6236>.

[4] Rider WJ, Kothe DB. Reconstructing volume tracking. J Comput Phys 1998;141(2):112–52. http://dx.doi.org/10.1006/jcph.1998.5906. <http://dx.doi.org/10.1006/jcph.1998.5906>.

[5] Hou TY, LeFloch PG. Why nonconservative schemes converge to wrong solutions: error analysis. Math Comput 1994;62(206):497–530. http://dx.doi.org/10.2307/2153520. <http://dx.doi.org/10.2307/2153520>.

[6] Wang C, Shu C-W. An interface treating technique for compressible multi-medium flow with Runge–Kutta discontinuous Galerkin method. J Comput Phys 2010;229(23):8823–43. http://dx.doi.org/10.1016/j.jcp.2010.08.012. UR. <http://dx.doi.org/10.1016/j.jcp.2010.08.012>.

[7] Rhebergen S, Bokhove O, van der Vegt JJW. Discontinuous Galerkin finite element methods for hyperbolic nonconservative partial differential equations. J Comput Phys 2008;227(3):1887–922. http://dx.doi.org/10.1016/j.jcp.2007.10.007. <http://dx.doi.org/10.1016/j.jcp.2007.10.007>.

[8] Dumbser M, Hidalgo A, Castro M, Parés C, Toro EF. FORCE schemes on unstructured meshes II: non-conservative hyperbolic systems. Comput Methods Appl Mech Eng 2010;199(9-12):625–47. http://dx.doi.org/10.1016/j.cma.2009.10.016. <http://dx.doi.org/10.1016/j.cma.2009.10.016>.

[9] Abgrall R, Saurel R. Discrete equations for physical and numerical compressible multiphase mixtures. J Comput Phys 2003;186:361–96.

[10] Baer M, Nunziato J. A two-phase mixture theory for the deflagration-to-detonation transition (ddt) in reactive granular materials. Int J Multiphase Flows 1986;12(12):861–89.

[11] Dal Maso G, Lefloch PG, Murat F. Definition and weak stability of nonconservative products. J Math Pures Appl (9) 1995;74(6):483–548.

[12] Andrianov N, Warnecke G. The Riemann problem for the Baer–Nunziato two-phase flow model. J Comput Phys 2004;195(2):434–64. http://dx.doi.org/10.1016/j.jcp.2003.10.006. <http://dx.doi.org/10.1016/j.jcp.2003.10.006>.

[13] Drew D, Passman S. Theory of multicomponent fluids. Applied mathematical sciences, vol. 13. New York: Springer-Verlag; 1999.

[14] Cockburn B, Shu C-W. Runge–Kutta discontinuous Galerkin methods for convection-dominated problems. J Sci Comput 2001;16(3):173–261. http://dx.doi.org/10.1023/A:1012873910884. <http://dx.doi.org/10.1023/A: 1012873910884>.

[15] Zhang X, Shu C-W. On maximum-principle-satisfying high order schemes for scalar conservation laws. J Comput Phys 2010;229(9):3091–120. http://dx.doi.org/10.1016/j.jcp.2009.12.030. <http://dx.doi.org/10.1016/j.jcp.2009.12.030>.

[16] Liu X-D, Osher S. Nonoscillatory high order accurate self-similar maximum principle satisfying shock capturing schemes. I. SIAM J Numer Anal 1996;33(2):760–79. http://dx.doi.org/10.1137/0733038. <http://dx.doi.org/10.1137/0733038>.

[17] Bermudez A, Vazquez ME. Upwind methods for hyperbolic conservation laws with source terms. Comput Fluids 1994;23(8):1049–71. http://dx.doi.org/10.1016/0045-79394)90004-3. <http://dx.doi.org/10.1016/0045-7930(94)90004-3>.

[18] Xing Y, Shu C-W. High order well-balanced finite volume WENO schemes and discontinuous Galerkin methods for a class of hyperbolic systems with source terms. J Comput Phys 2006;214(2):567–98. http://dx.doi.org/10.1016/j.jcp.2005.10.005. <http://dx.doi.org/10.1016/j.jcp.2005.10.005>.

[19] Zalesak ST. Fully multidimensional flux-corrected transport algorithms for fluids. J Comput Phys 1979;31(3):335–62.